Electronic Supplementary Information (ESI) for:

Injectable zwitterionic thermosensitive hydrogels with low-protein adsorption and combined effect of photothermal-chemotherapy†

Anbi Zheng,[a,1] Di Wu,[a,1] Man Fan,[a,1] Hong Wang,[a] Yonggui Liao,[a] Qin Wang,*[a] and Yajiang Yang[a]

Hubei Key Laboratory of Bioinorganic Chemistry & Materia Medica, School of Chemistry and Chemical Engineering, Huazhong University of Science and Technology, Wuhan 430074, People's Republic of China

Chemical structure characterization of PNS nanogels

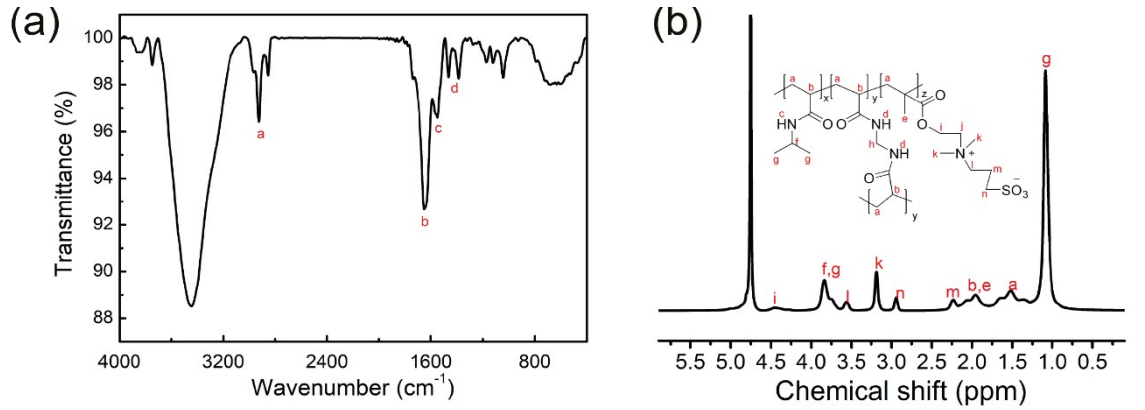

Fig. S1 (a) FT-IR spectrum and (b) ^{1}H NMR spectrum of PNS nanogels.

The copolymerization of SBMA, NIPAM and MBA was confirmed by FTIR and ^{1}H NMR spectrum. In Fig. S1a, the peak at 2924 cm^{-1} (peak a) is assigned to C–H stretching vibrations of methyl or methylene in polymer. The peak at 1649 cm^{-1} (peak b) is assigned to C=O stretching of amide and 1462 cm^{-1} (peak c) is assigned to C–N bond of amine. The stretching bands of S=O in SBMA appears at 1044 cm^{-1} (peak e). ^{1}H NMR spectrum was shown in Fig. S1b. The peaks at δ=1.48~1.60 (a) and δ=1.91~2.01 (b) were assigned to methylene (a) and methylidyne (b) produced from the polymerization of carbon-carbon double bonds, respectively. The others are assigned as follows: δ=1.1 (g, $CH(C\mathbf{H}_3)_2$), 2.2 (m, $C\mathbf{H}_2CH_2SO_3^-$), 2.89 (n, $CH_2C\mathbf{H}_2SO_3^-$), 3.16 (k, $N^+(C\mathbf{H}_3)_2$), 3.52 (l，$N^+C\mathbf{H}_2CH_2CH_2SO_3^-$), 3.71 (j，$COOCH_2C\mathbf{H}_2$), 3.79 (f，$C\mathbf{H}(CH_3)_2$), 4.41 (i, $COOC\mathbf{H}_2$; h, $CONHC\mathbf{H}_2NHCO$).

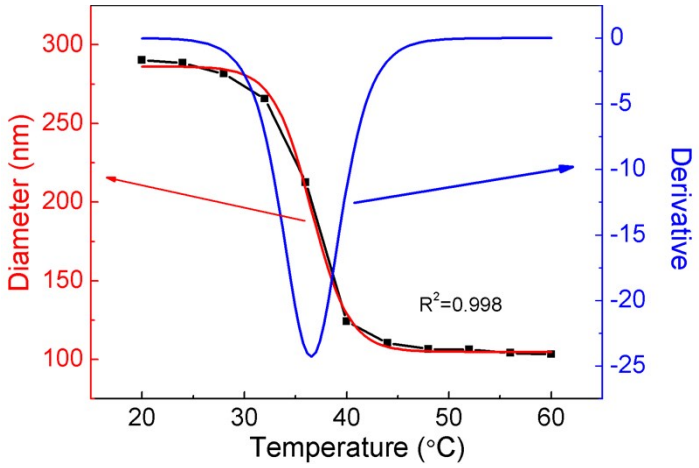

Fig. S2 Diameters of PNA nanogels *versus* temperature.

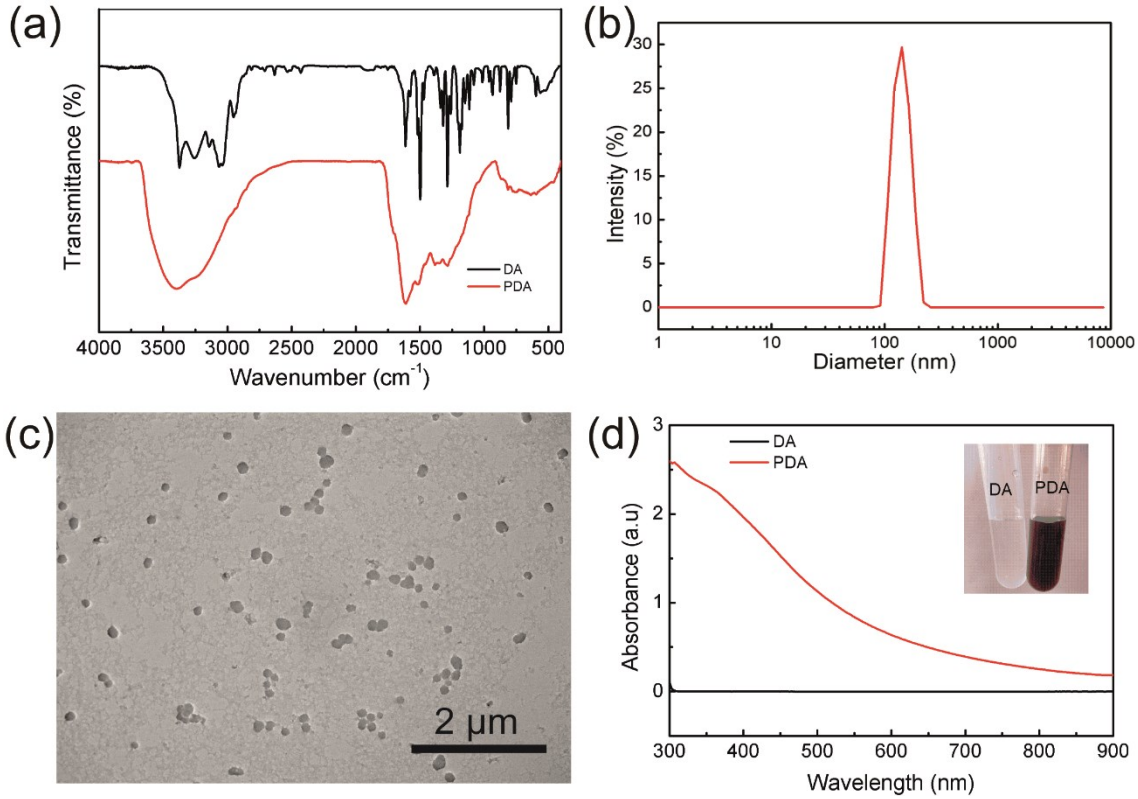

Fig. S3 (a) FT-IR spectra of PDA NPs. (b) Hydrodynamic diameter of PDA NPs and its distribution measured by DLS. (c) TEM image of PDA NPs and (d) UV-Vis-NIR spectra of PDA NPs aqueous suspension and DA aqueous solution (both the concentration of DA and PDA NPs were 200 μg/mL).

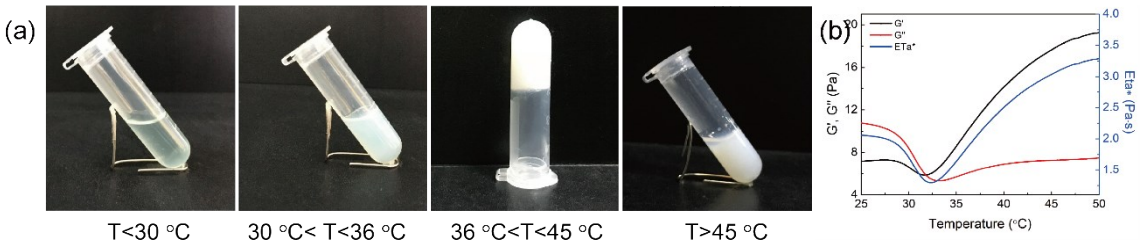

Fig. S4 (a) Photographs and (b) rheology behavior of the sol-gel transition of PNS dispersion (25 wt%).

Photothermal conversion efficiency of PDA NPs

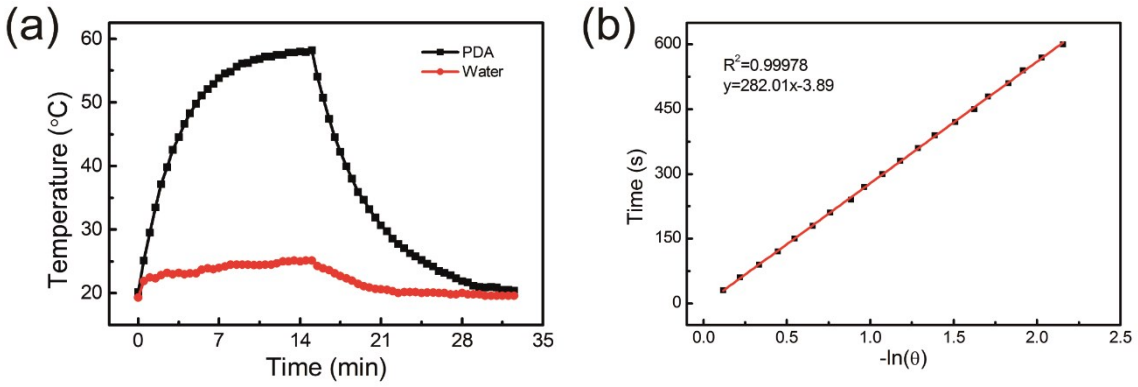

Fig. S5 (a) Temperature change curve of PDA NPs dispersion (200 μg/mL) under NIR laser irradiation (808 nm, 1.0 W/cm^2) for 15 min and then shutting off the laser, and (b) linear relationship of time *versus* $-ln\theta$ obtained from the cooling curve in (a).

The photothermal conversion efficiency (η) of PDA NPs can be calculated according to Eq. S1 as reported [1,2] and the experimental data.

$$\eta = \frac{hA\Delta T_{max} - Q_s}{I(1 - 10^{-A_\lambda})} \qquad \textbf{(Eq. S1)}$$

Wherein h is the heat transfer coefficient, A is the surface area of the container, ΔT_{max} is the maximum temperature change of PDA NPs suspension at the steady-state temperature, I is the laser power density used, A_λ is the absorbance of the PDA NPs suspension at 808 nm, and Qs is the heat of the solvent (water) produced by the laser irradiation.

In this system, ΔT_{max} was 38.0 °C (Fig. S5a), A_λ was 0.237 (Fig. S3d, l=1 cm) and I was 1.0 W/cm^2. Q_s could be calculated from $Q_s = C_{water}\, m\Delta T/t$ = 4.2 J/(g·°C) × 0.30 g × 5.8 °C/900 s =8.12 mW. hA was obtained by applying the linear time data from the cooling period *vs* $-ln\theta$ (Fig. S5b) and Eq. S2. Herein, θ is defined in Eq. S3, m and Cp are the mass (0.30 g) and heat capacity of water (4.2 J/(g·°C)).

$$\tau_s = \frac{\sum_i m_i\, c_{p,i}}{hA} \qquad \textbf{(Eq. S2)}$$

$$\theta = \frac{\Delta T}{\Delta T_{max}} = \frac{T - T_{surr}}{T_{max} - T_{surr}} \qquad \textbf{(Eq. S3)}$$

According to the data in Fig. S5a and Eq. 3, $-ln\theta$ at different time could be calculated out. In addition, the slope of the fitted line in Fig. S5b was the time constant τ_s (281.01). Therefore, hA equaled to 4.48 mW/°C according to Eq. S2 and η was 38.5% based on Eq. S1.

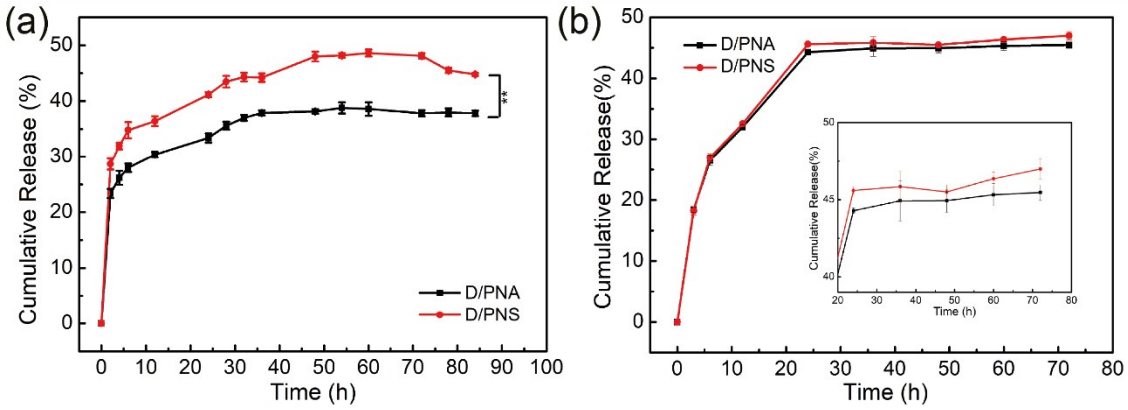

Fig. S6 *In vitro* DOX release profiles of D/PNS and D/PNA hydrogels. (a) Without and (b) with FBS adsorbed on the DOX-loaded hydrogel (n=3). Note: ** P<0.01, with significant difference.

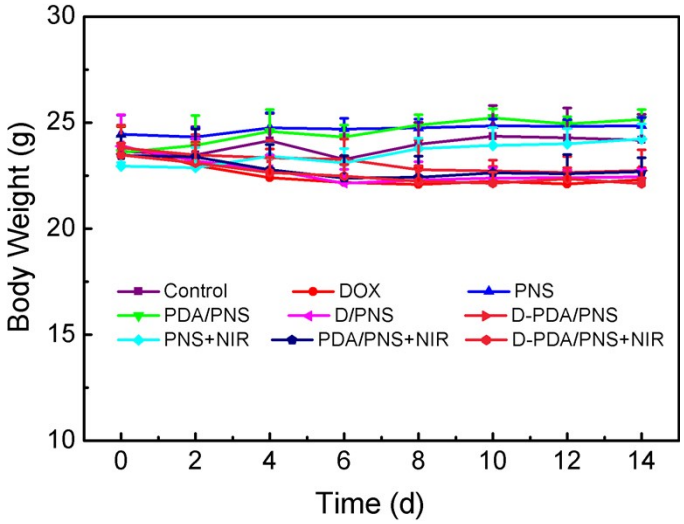

Fig. S7 Body weight of mice *versus* time.

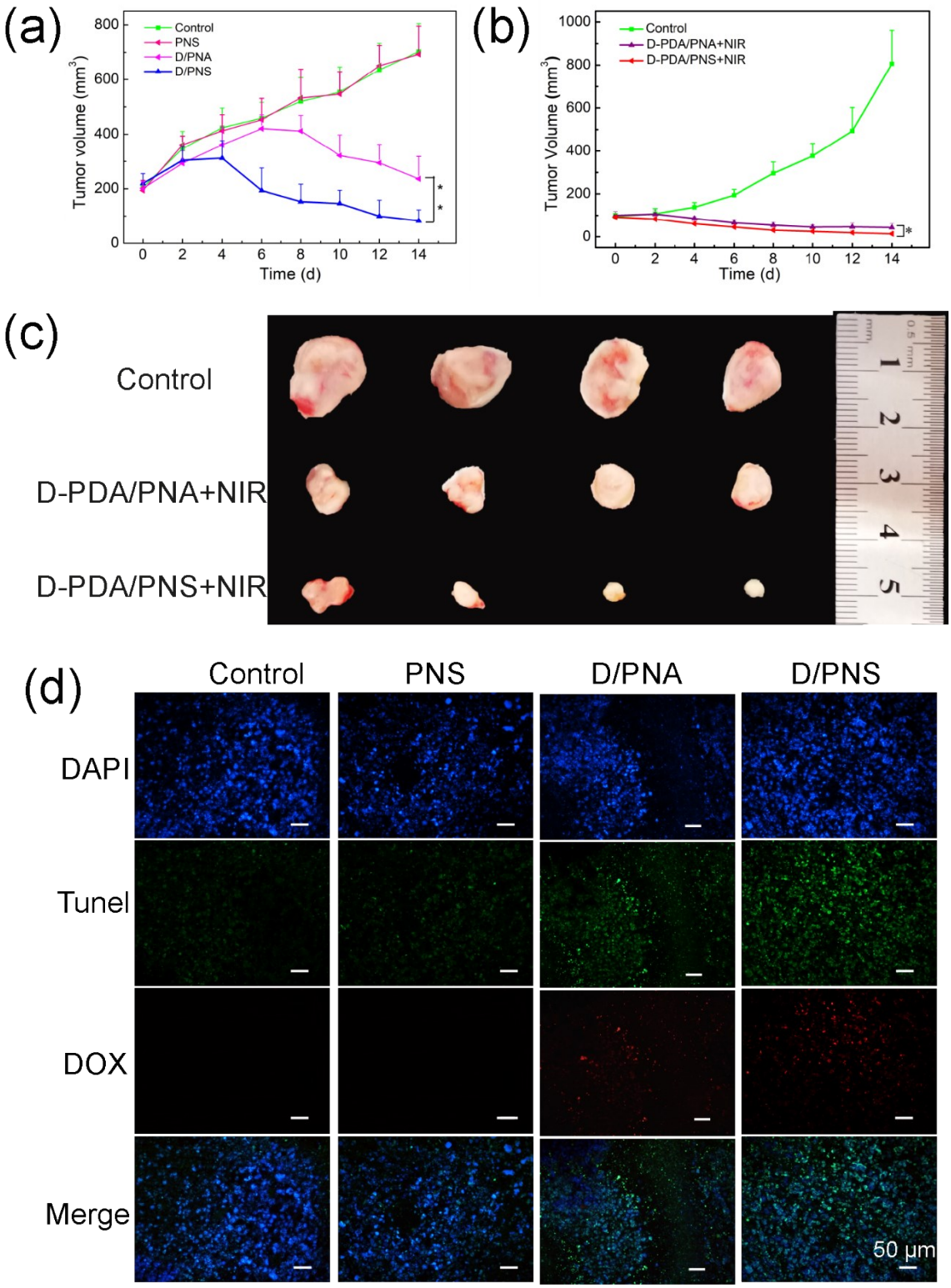

Fig. S8 *In vivo* anti-tumor effect. (a) Tumour volumes change of D/PNS compared with D/PNA versus time. (b) Tumour volumes change of D-PDA/PNS compared with D-PDA/PNA *versus* time and (c) the corresponding photographs of the peeled tumours after intratumoral injection for 14 days. (d) Fluorescence

images of tumour tissue slice stained by Tunel. **P<0.01, *P<0.05.

References

1 Y. Gao, X. Wu, L. Zhou, Y. Su and C. M. Dong, *Macromol. Rapid. Comm.*, 2015, **36**, 916–922.

2 Y. L. Liu, K. L. Ai, J. H. Liu, M. Deng, Y. Y. He and L. H. Lu, *Adv. Mater.*, 2013, **25**, 1353–1359.